

## First measurement of $f_0(980)$ meson photoproduction in the $\pi^0\pi^0$ decay mode

Unlike ordinary hadrons (such as protons, neutrons, and pions) containing only two ( $q\bar{q}$ ) or three ( $qqq$ ) quarks, exotic hadrons belong to a group of special subatomic particles that consist of more than three valence quarks. As quantum chromodynamics (QCD), the most acceptable theory of strong forces that determines the behavior of subatomic particles, does not limit the number of quarks in a hadron, searching for exotic hadrons and studying their structures are important for improving our understanding of strong interaction mechanisms.

Experimental searches for exotic hadrons have been conducted over several years. In the BGOegg experiment conducted at SPRING-8 BL31LEP, we attempted to understand the structure of the scalar meson  $f_0(980)$  because it has attracted attention as a possible candidate for exotic non  $q\bar{q}$  states, such as a  $K\bar{K}$  molecule and tetraquark. Differential cross sections and photon beam asymmetries in  $f_0(980)$  photoproduction were measured to determine their nature [1]. Differential cross sections may more effectively reflect the strength of  $q\bar{q}$  and  $K\bar{K}$  components in  $f_0(980)$ , as predicted by a Regge model calculation mainly with the exchange of vector mesons, such as  $\rho$  and  $\omega$  [2]. Photon beam asymmetry ( $\Sigma$ ) measurement was performed to study the  $t$ -channel vector meson exchange mechanism, predicted to give  $\Sigma = -1$  in the scalar meson photoproduction [3]. The  $\Sigma$  value decreases if contaminated by unnatural parity processes.

In the BGOegg experiment, a linearly polarized photon beam was produced via laser Compton scattering at BL31LEP and tagged in the energy region of 1.3–2.4 GeV. To detect final-state neutral and charged particles, the  $4\pi$  electromagnetic calorimeter BGOegg and several charged-particle detectors were employed at the LEPS2 experimental building [1]. This calorimeter, comprising 1320  $\text{Bi}_4\text{Ge}_3\text{O}_{12}$  (BGO) crystals assembled in 22 layers, had a coverage of  $24^\circ$  to  $144^\circ$  in the polar angle and full region in the azimuthal angle, providing the world's-best energy resolution of 1.4% for a 1-GeV  $\gamma$ -ray. The photon beam was irradiated onto a 54-mm-long liquid hydrogen target to produce  $f_0(980)$  mesons, and the reaction products were detected using the BGOegg calorimeter surrounding the target. Thirty bars of plastic scintillators were placed between the target and the calorimeter to identify the charged particles. In the very forward region ( $\theta < 21^\circ$ ), a planar drift chamber was placed to detect the charged particles.

The  $f_0(980)$  meson was identified by detecting all the final-state particles of the reaction  $\gamma p \rightarrow f_0(980)p \rightarrow \pi^0\pi^0 p \rightarrow 4\gamma p$ . The measurement of differential cross sections and photon beam asymmetries for this reaction in this study is the first attempt in the world. As a major advantage, the  $f_0(980) \rightarrow \pi^0\pi^0$  process is free of  $\rho$ -meson photoproduction, which is in contrast a dominant background contribution in the case of identifying  $f_0(980)$  mesons in the  $\pi^+\pi^-$  decay mode.

In the event selection, four  $\gamma$ -rays were detected by the BGOegg calorimeter as neutral particles greater than the 30 MeV threshold, and the timing difference of any two  $\gamma$ -rays was required to be less than 2 ns to reduce the background owing to accidental hits. The most forward or most backward layer of the calorimeter was not used for  $\gamma$  detection to avoid a large energy leak. A proton was detected as a charged cluster in a calorimeter or as a straight track in a planar drift chamber. A kinematic fit with the constraints of four-momentum conservation and  $\pi$  mass was also used to inspect the selected events, and only the events with  $\chi^2$  probabilities greater than 2% were retained to reduce background events.

The  $f_0(980)$  signal was extracted from the  $\pi^0\pi^0$  invariant mass ( $M(\pi^0\pi^0)$ ) distribution, plotted at photon beam energies beyond its production threshold of 1450 MeV. To suppress background events owing to  $\Delta(1232)$  photoproduction, the cut for the  $\pi^0 p$  invariant mass was used:  $[M(\pi^0 p) - 1232] > 50 \text{ MeV}/c^2$ , where only a lower momentum  $\pi^0$  was combined with a proton. After this cut, the  $f_0(980)$  signal was clearly observed in the  $\pi^0\pi^0$  invariant mass distributions

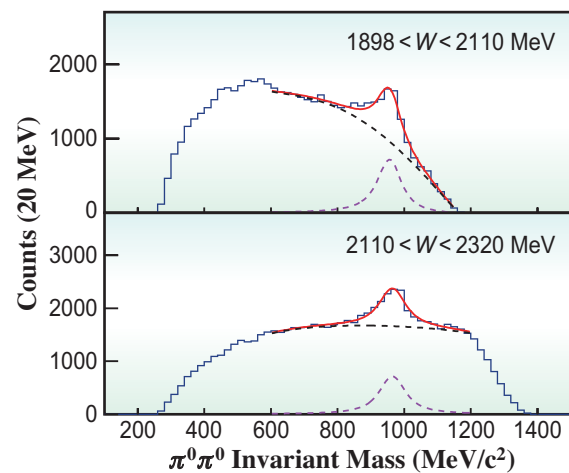


Fig. 1. Invariant mass spectra of  $\pi^0\pi^0$  in two energy bins. Voigt functions are fitted with polynomial background functions to extract  $f_0(980)$  signals.

both in the higher ( $2110 < W < 2320$  MeV) and lower ( $1898 < W < 2110$  MeV) total-energy ( $W$ ) regions, as shown in Fig. 1. The  $f_0(980)$  signal was separated from background events by fitting a Voigt function (representing a  $f_0(980)$  component) in conjunction with a fourth-order polynomial function to the  $M(\pi^0\pi^0)$  spectra.

The yield of the fitted  $f_0(980)$  signal was obtained by integrating the Voigt function with the fitted scale factors. After being corrected by geometrical acceptance and detection efficiencies estimated using MC simulations, the differential cross sections  $d\sigma/d\Omega$  of the reaction  $\gamma p \rightarrow f_0(980)p \rightarrow \pi^0\pi^0 p$  were measured as a function of  $\cos\theta_{f_0}^{c.m.}$  in both the higher and lower  $W$  regions.  $d\sigma/d\Omega$  was observed to be nearly flat in the lower  $W$  region, whereas an enhancement at  $\cos\theta_{f_0}^{c.m.} \geq 0$  appeared in the higher  $W$  region, indicating the increase of  $t$ -channel contributions. Differential cross sections  $d\sigma/dt$  were also measured as shown in Fig. 2 and compared with a theoretical prediction [2]. The  $d\sigma/dt$  values in a small  $|t|$  region were comparable to the theoretical prediction assuming a  $q\bar{q}$  component in  $f_0(980)$ .

In addition, photon beam asymmetries  $\Sigma$  were measured by evaluating  $f_0(980)$  signal yields in two azimuthal angle ( $\Phi$ ) regions relative to the linear polarization vector of a photon beam: 1) parallel region,  $-\pi/4 < \Phi < \pi/4$  and  $3\pi/4 < \Phi < 5\pi/4$ ; 2) perpendicular region,  $\pi/4 < \Phi < 3\pi/4$  and  $5\pi/4 < \Phi < 7\pi/4$ . The  $\Sigma$  value was obtained by the relation  $(P_\gamma \Sigma)/f_{int} = (N_\perp - N_\parallel)/(N_\perp + N_\parallel)$ , where  $P_\gamma$  is the photon beam polarization (determined to be 0.677 and 0.895 for the lower and higher  $W$  regions, respectively),  $N_\perp$  is the yield in the perpendicular region,  $N_\parallel$  is the yield in the parallel region, and  $f_{int} = \pi/2$  is a correction factor for the integration over  $\pi/2$  azimuthal angle ranges.

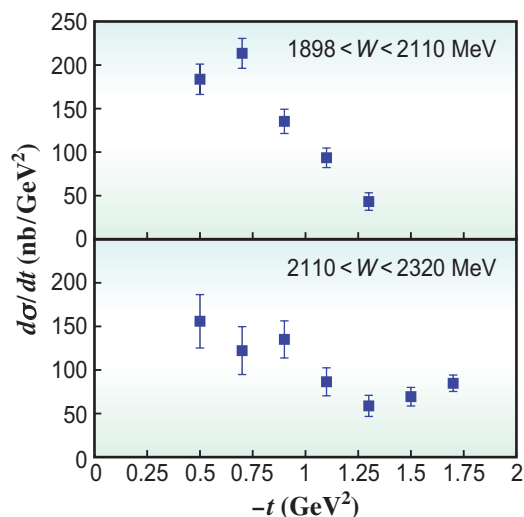


Fig. 2. Differential cross sections  $d\sigma/dt$  of  $\gamma p \rightarrow f_0(980)p \rightarrow \pi^0\pi^0 p$ .

As shown in Fig. 3, the  $\Sigma$ s in the lower  $W$  bin are close to zero or slightly positive, whereas in the higher bin, they are negative values around  $-0.3$ , indicating the contribution of  $t$ -channel vector meson (natural parity) exchange in  $f_0(980)$  photoproduction. At the higher energies, the deviation from  $\Sigma = -1$  is observed possibly because of the unnatural parity contribution of axial-vector exchange (e.g.,  $b_1(1235)$ ) in addition to the contamination of  $s$ - and  $u$ -channel diagrams.

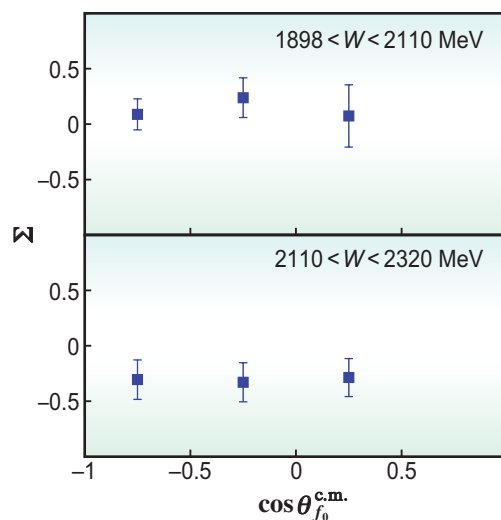


Fig. 3. Photon beam asymmetries  $\Sigma$  of the reaction  $\gamma p \rightarrow f_0(980)p$ .

Qinghua He<sup>a,\*</sup> and Norihito Muramatsu<sup>b</sup>

<sup>a</sup> Department of Nuclear Science and Technology, Nanjing University of Aeronautics and Astronautics, China

<sup>b</sup> Research Center for Electron Photon Science, Tohoku University

\*Email: heqh@nuaa.edu.cn

### References

- [1] N. Muramatsu, S. K. Wang, Q. H. He, J. K. Ahn, W. C. Chang, J. Y. Chen, M. L. Chu, S. Daté, T. Gogami, H. Goto, H. Hamano, T. Hashimoto, K. Hicks, T. Hiraiwa, Y. Honda, T. Hotta, H. Ikuno, Y. Inoue, T. Ishikawa, I. Jaegle, J. M. Jo, Y. Kasamatsu, H. Katsuragawa, S. Kido, Y. Kon, S. Masumoto, Y. Matsumura, M. Miyabe, K. Mizutani, T. Nakamura, T. Nakano, T. Nam, M. Niiyama, Y. Nozawa, Y. Ohashi, H. Ohnishi, T. Ohta, M. Okabe, K. Ozawa, C. Rangacharyulu, S. Y. Ryu, Y. Sada, T. Shibukawa, H. Shimizu, R. Shirai, K. Shiraishi, E. A. Stokovskiy, Y. Sugaya, M. Sumihama, S. Suzuki, S. Tanaka, Y. Taniguchi, A. Tokiyasu, N. Tomida, Y. Tsuchikawa, T. Ueda, T. F. Wang, H. Yamazaki, R. Yamazaki, Y. Yanai, T. Yorita, C. Yoshida, M. Yosoi: *Phys. Rev. C* **107** (2023) L042201.
- [2] A. Donnachie and Y. S. Kalashnikova: *Phys. Rev. C* **93** (2016) 025203.
- [3] I. I. Strakovskiy *et al.*: *Phys. Rev. C* **107** (2023) 015203.